# $Fe_3O_4$-Functionalized UiO-66 with Facile Magnetic Recovery for High-Capacity and Rapid Uranium Removal from Contaminated Aqueous Solutions

*Yunhu Hu [1,2], Zilong Chen[2], Dunpeng You[2], Renpeng Tu[2], Mai Xu[2], Jianfeng Zhang[2], Jing Zhao[2], Mu You [1,3*]*

[1]*Engineering Technology Research Center of Coal Resources Comprehensive Utilization, Huainan, Anhui 232001, P.R. China*

[2]*School of Chemistry and Material Engineering, Huainan Normal University, Huainan, Anhui 232038, P.R. China*

[3]*School of Biology Engineering, Huainan Normal University, Huainan, Anhui 232038, P.R. China*

**Corresponding author*:

*Email address: youmu@ustct.edu.cn (M. You)*

**Materials:**

Zirconium chloride ($ZrCl_4$), terephthalic acid ($H_2BDC$), N-N dimethylformamide (DMF), triffuoroacetic acid (TFA), Methanol, urea ($H_2NCONH_2$), iron (III) chloride hexahydrate ($FeCl_3·6H_2O$), trisodium citrate ($C_6H_5Na_3O_7·2H_2O$), polyacrylamide (PAM, $[CH_2CH(CONH_2)]_n$), and ethanol (EtOH) are analytical grade and used without further purification. All chemicals were purchased from Sinopharm Chemical Reagent Co. Ltd.

**Characterization**

The surface morphology of the as-prepared samples was characterized using a ZEISS G300 field-emission scanning electron microscope (FE-SEM). The crystal structure was determined by a Philips X'pert PRO X-ray diffractometer (XRD). Thermal stability tests were performed on a DTG-60H thermogravimetric analyzer, where thermogravimetric analysis (TGA) was carried out in an air atmosphere from room temperature to 500°C. X-ray photoelectron spectroscopy (XPS) data were collected using a Thermo VG Scientific ESCALAB250 photoelectron spectrometer to analyze elemental composition and chemical states. Magnetic hysteresis (M-H) loops of the samples were measured at room temperature with a Quantum Design Corp MPMS XL5 magnetometer.

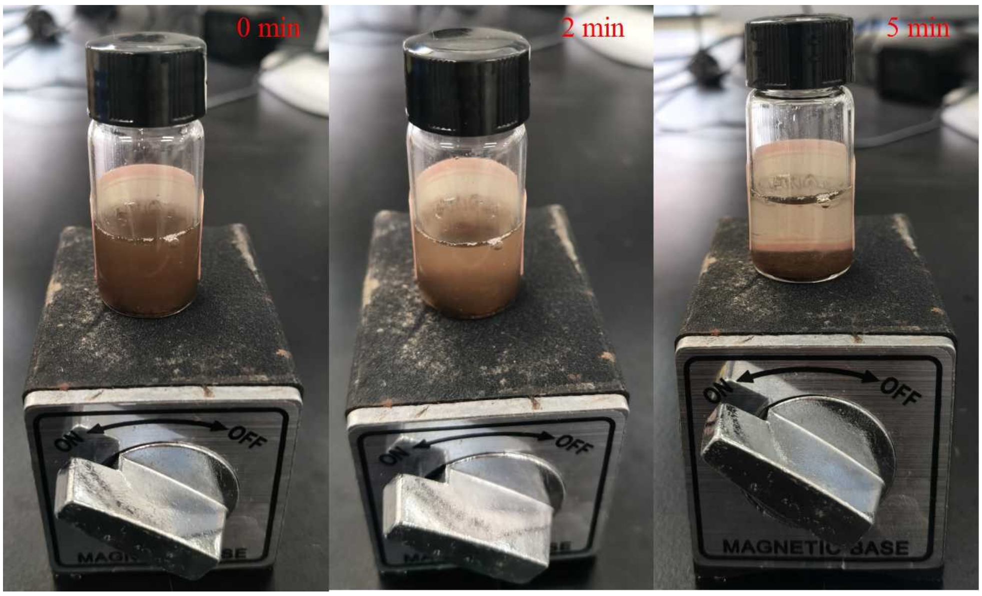

**Figure S1.** Photograph of the magnetic separation process of $Fe_3O_4$@UiO-66.

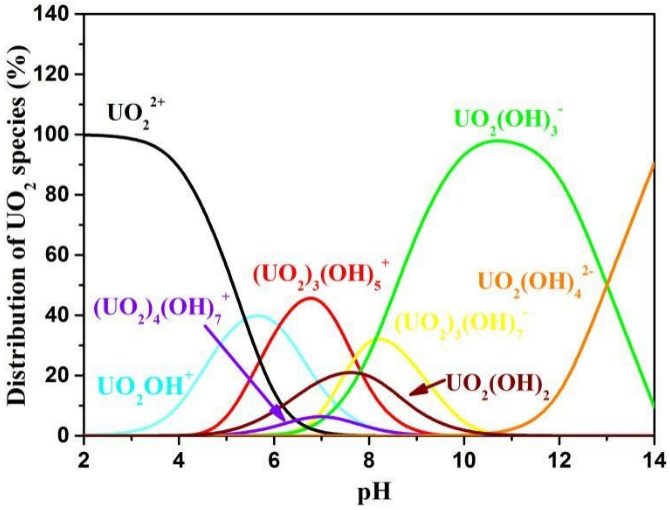


**Figure S2.**The relative distribution of U (VI) species as a function of pH in aqueous solutions.

**Table S1.** Equations and nomenclatures of the two isotherm models ($C_e$ (mg/L) and $Q_e$ (mg/g) refer to the U(VI) concentration and the adsorption capacity at equilibrium, respectively).

| Equations | Nomenclatures | |
|---|---|---|
| $Q_e = \frac{bC_eQ_{max}}{bC_e + 1}$ | $b$(L/g) | Langmuir constant related to the free energy for adsorption |
| | $Q_{max}$(mg/g) | Langmuir monolayer adsorption capacity |
| $Q_e = K_f C_e^{1/n}$ | $K_f$(mol$^{1-n}$L$^n$/g) | Freundlich constant of the relative adsorption capacity of the EIR |
| | $n$ | Freundlich constant of the heterogeneity factor |

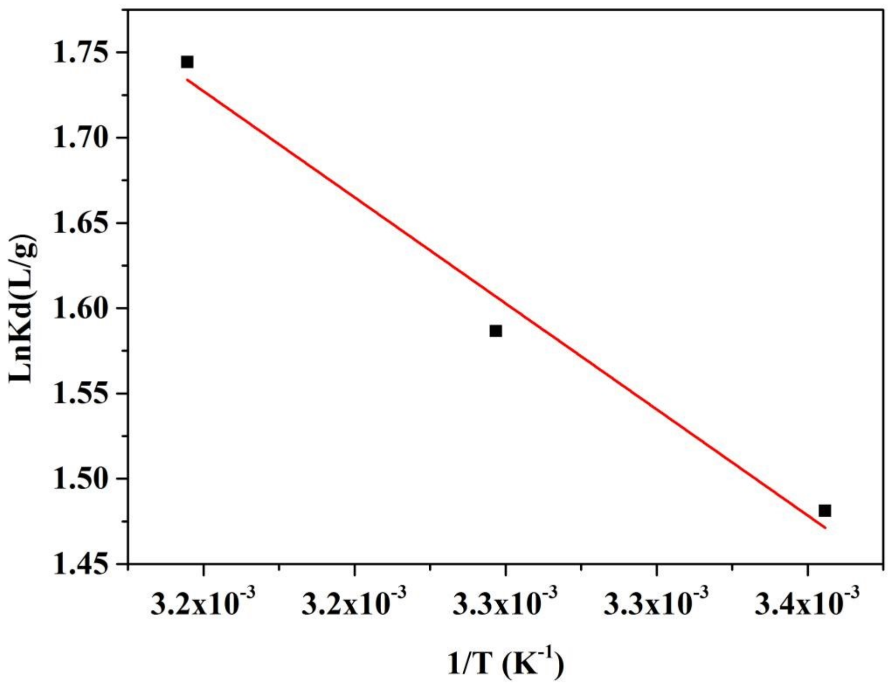


**Figure S3.** The plot of 1/T versus $\ln K_d$ (pH=8.0, t=24 h).

**Table S2.** Thermodynamic parameters for the U(VI) adsorption process on $Fe_3O_4$@UiO-66.

| T (K) | $\Delta G^0$ (kJ/mol) | $\Delta H^0$ (kJ/mol) | $\Delta S^0$ (J/mol·K) |
|---|---|---|---|
| 298.15 | -3.67 | 4.58 | 27.68 |
| 308.15 | -4.06 | | |
| 318.15 | -4.61 | | |

**Table S3.** Equations and nomenclatures of the three kinetic models ($Q_e$ and $Q_t$ refer to the amounts of U(VI) adsorbed at equilibrium and designed time t, respectively).

| Equations | Nomenclatures |
|---|---|

| | | |
|---|---|---|
| $Q_t = Q_e(1 - e^{-k_1 t})$ | $k_1$ ($min^{-1}$) | Pseudo-first-order rate constant |
| $\frac{t}{Q_t} = \frac{1}{2k_2 Q_e^2} + \frac{t}{Q_e}$ | $k_2$ (g/mg·min) | Pseudo-second-order rate constant |
| $Q_t = k_i\sqrt{t} + C$ | $k_i$ (mg/g·$min^{1/2}$) | Intra-particle diffusion constant |
| | $C$ | Intercept in the intra-particle diffusion model |

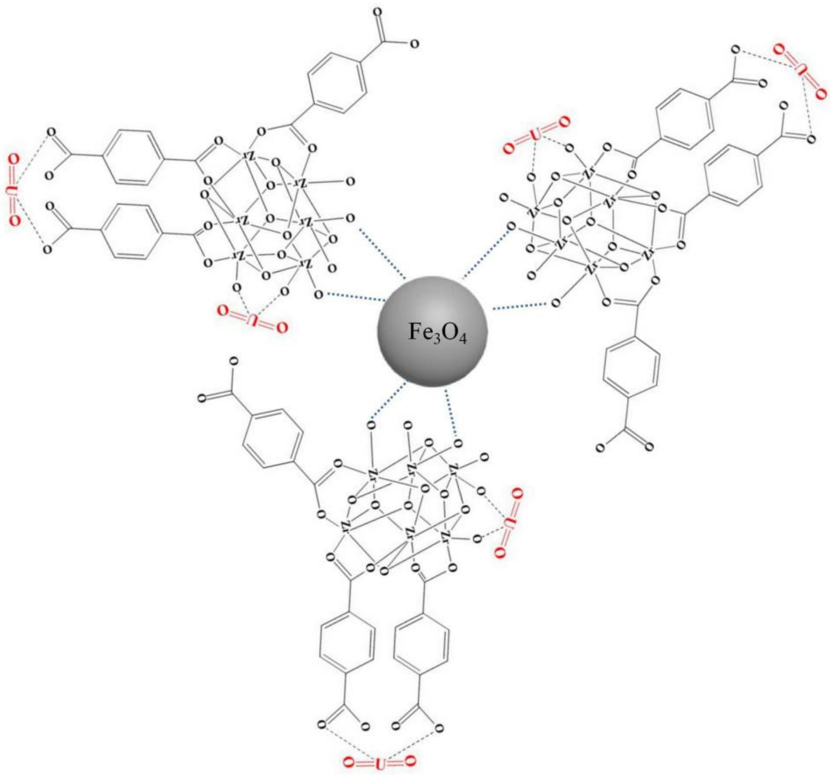


**Figure S4.** Schematic diagram of the mechanism of Zr-$O^-$ complexation with U(VI).